Human Molecular Genetics, 2005, Vol. 14, No. 14 ***1977–1989***
doi:10.1093/hmg/ddi203
Advance Access published on May 25, 2005

Identification of quantitative trait loci controlling cortical motor evoked potentials in experimental autoimmune encephalomyelitis: correlation with incidence, onset and severity of disease

Ignacio Mazón Peláez[1,†], Susanne Vogler[1,†], Ulf Strauss[2], Patrik Wernhoff[1], Jens Pahnke[2,4], Gudrun Brockmann[3], Holger Moch[4], Hans-Juergen Thiesen[1], Arndt Rolfs[2] and Saleh M. Ibrahim[1,*]

[1]Department of Immunology and [2]Department of Neurology, University of Rostock, Schillingallee 70, 18055 Rostock, Germany, [3]Institute of Animal Science, Humboldt University, Berlin, Germany and [4]Department of Pathology, Institute of Clinical Pathology, University Hospital Zürich, Switzerland

Received January 26, 2005; Revised March 24, 2005; Accepted May 23, 2005

Experimental autoimmune encephalomyelitis (EAE) is a polygenic chronic inflammatory demyelinating disease of the nervous system, commonly used as an animal model of multiple sclerosis. Previous studies have identified multiple quantitative trait loci (QTLs) controlling different aspects of disease pathogenesis. However, direct genetic control of cortical motor evoked potentials (cMEPs) as a straightforward measure of extent of demyelination or synaptic block has not been investigated earlier. Here, we examined the genetic control of different traits of EAE in a F2 intercross population generated from the EAE susceptible SJL/J (SJL) and the EAE resistant C57BL/10.S (B10.S) mouse strains involving 400 animals. The genotypes of 150 microsatellite markers were determined in each animal and correlated to phenotypic data of onset and severity of disease, cell infiltration and cMEPs. Nine QTLs were identified. Three sex-linked QTLs mapped to chromosomes 2, 10 and 18 linked to disease severity in females, whereas QTLs on chromosomes 1, 8 and 15 linked to the latency of the cMEPs. QTLs affecting T-lymphocyte, B-lymphocyte and microglia infiltration mapped on chromosomes 8 and 15. The cMEP-associated QTLs correlated with incidence, onset or severity of disease, e.g. QTL on chromosome 8, 32–48 cM (EAE 31) (LOD 6.9, $P < 0.001$), associated to cMEP latencies in non-immunized mice and correlated with disease onset and EAE 32 on chromosome 15 linked to cMEP latencies 15 days post-immunization and correlated with disease severity. Additionally, applying tissue microarray technology, we identified QTLs associated to microglia and lymphocytes infiltration on chromosomes 8 and 15, which are different from the QTLs controlling cMEP latencies. There were no alterations in the morphological appearance of the myelin sheaths. Our findings suggest a possible role of myelin composition and/or synaptic transmission in susceptibility to EAE.

INTRODUCTION

Multiple sclerosis (MS) is a complex polygenic disease with prevalence dependent on age, gender and hormonal and environmental factors. Susceptibility to MS is influenced by genetic factors, as indicated by numerous studies showing higher rates of disease concordance in monozygotic than in dizygotic twins, and higher incidence in the offspring of MS patients (1,2). The primary genetic contribution to MS susceptibility is thought to be linked to the HLA locus (1). Identification of the non-MHC genetic loci regulating MS is a complex task due to genetic heterogeneity, incomplete penetrance and influence of environmental factors (3,4). Hence, genetic analysis of well-defined experimental models

*To whom correspondence should be addressed. Tel: +49 3814945872; Fax: +49 3814945882; Email: saleh.ibrahim@med.uni-rostock.de
†The authors wish it to be known that, in their opinion, the first two authors should be regarded as joint First Authors.

such as experimental autoimmune encephalomyelitis (EAE) and the search of syntenic regions between different species in these susceptible loci (5) have the potential to accelerate the genetic analysis of MS (6). In animals and humans, most studies indicate that both non-MHC genes and MHC genes are associated with the susceptibility to EAE (7). The first quantitative trait loci (QTL) identified, EAE1, is located on chromosome 17 and includes the MHC. Nevertheless, inbred strains sharing the same MHC haplotype vary in their susceptibility, indicating the existence of non-MHC susceptibility genes. The conservative estimate for the number of non-MHC susceptibility genes involved is suggested to be more than 30 (8–10). In the past few years, extensive search localized 28 QTLs that regulate EAE in mice, mostly in crosses involving the SJL/J and C57BL/10.S strains, both sharing the same H2 haplotype (11).

We assumed that there could be additional QTLs that contribute to the susceptibility to EAE by controlling disease pathways that have not yet been identified. So we set out to identify such QTLs in a new wide genome screen of the F2 generation between C57BL/10.S and SJL/J strains. We focused on functional parameters of the central nervous system (CNS) of EAE mice as a primary trait. Impaired function reflected in electrophysiological changes was shown to be associated with disease severity and demyelination in earlier studies (12). The deterioration of the myelin sheath is one of the main pathological characteristics during the disease, and temporal dispersion of neuronal conduction due to demyelination can result in altered cortical evoked responses. Cortical motor evoked potentials (cMEP) provide quantitative data on the physiological status of myelinated cortical motor neuron projections and synaptic transmission and are thus particularly appropriate for a functional study of the descending tracts. With the measurement of latencies of cMEP, additional features such as cell infiltration in the spinal cord, demyelination and axonal damage by implementing tissue microarrays (TMAs) of spinal cord cylinders, disease onset and severity were performed. In this study, we report the identification of nine QTLs controlling disease severity, cellular infiltration and latencies of cMEPs.

RESULTS

EAE incidence and severity in (SJL/J-C57Bl/10S) F2 progeny

We generated a total number of 42 (SJL/J × C57BL/10.S) F1 and 400 (SJL/J × C57BL/10.S) F2 mice and immunized all of them. In the F1 progeny (SJL/J × C57BL/10.S), 82.8% (33 out of 42 animals) developed EAE, with a mean disease severity score of 2.75 ± 1.26 and a mean duration until onset of 13.04 ± 2.18 days. More females were affected (93.3%; 14 out of 15) than males (70.3%; 19 out of 27). The (SJL/J × C57BL/10.S) F2 animals had an incidence of 58.6% (248 out of 400), with a mean disease severity score of 2.69 ± 1.27 and a mean delay of onset of 12.98 ± 3.22 days post-immunization. Again, more females were affected (74.6%; 154 out of 207) than males (48.4%; 94 out of 193). This is consistent with published studies (10).

QTL associated with disease onset, severity and cell infiltration

We genotyped all F2 mice for linkage analysis, as described in Materials and Methods, and we phenotyped for the latencies of cMEP and cell infiltration in spinal cord, as well as disease onset and severity.

In the initial screen, we identified three QTLs controlling disease severity in females located on chromosomes 2, 10 and 18 (Table 1; Fig. 1). The first locus (EAE 33) on chromosome 2 had significant evidence of linkage to marker D2Mit32 (LOD score of 3.7). The second locus (EAE 34) on chromosome 10 was significantly linked to marker D10Mit261 (LOD score of 3.8). On chromosome 18, suggestive linkage to D18Mit144 was found (LOD score of 3.2). A QTL controlling disease onset in females on chromosome 10 with a peak linkage to a D10Mit271 was also identified (LOD score of 3.7). This locus overlaps with the severity controlling locus, EAE 34.

Additionally, we identified a suggestive QTL (EAE 38) associated to disease severity in males [linked to area under the curve (AUC) as a trait] on chromosome 15 (linked to D15Mit171, LOD score of 3.3).

Using TMAs and immunohistochemical stains for amyloid precursor protein (APP), myelin basic protein (MBP), neurofilament (NF200) and conventional Luxol–Nissl stain of spinal cords cylinders revealed no significant difference in the myelination pattern and axonal integrity, thus pointing towards a minor involvement of obvious demyelination at this stage of disease. However, the stains for microglia (IBA1) and B- and T-lymphocytes (B220 and CD3) revealed differences between the individual animals (Fig. 2). Two new QTLs related to the amount of infiltrating T-lymphocytes and microglia (Table 1; Fig. 3) were identified on chromosome 8 (EAE 36, linked to D8Mit259) and on chromosome 15 (EAE 37, linked to D15Mit35), respectively. A suggestive QTL associated to B-lymphocyte infiltration also map on chromosome 15 (EAE 38, linked to D15Mit171) in a region associated to severity in males.

To validate the loci, a two-point analysis (*F*-statistics, ANOVA) was performed (Supplementary Material, Table S2).

QTL associated with latencies of cMEP

In the light of the mismatch between severity and demyelination in the beginning of the disease, we sought to determine a direct functional measure as provided by cMEP.

The cMEP consists of a biphasic wave following the stimulus at a mean latency of 2.66 ms for fore limb and 3.95 ms for hind limb (Table 2). Interestingly, we observed differences in cMEP latencies between non-immunized parental strains (Table 2, $P < 0.05$), indicating that susceptible mice already have greater latencies in both hind limb and fore limb. There was a considerable prolongation of latencies (Table 2; Fig. 4) following disease induction in the F2 generation. A representative comparison between cMEP measured in a sick mouse at different time points during the disease is shown in Figure 4. As obvious, disease progression leads to a progressive delay in the cMEP onset accompanied by a scattering of the cMEP.

Table 1. Summary of the EAE linked quantitative trait loci identified in this study

QTL	Chromosome	Flanking markers	Effect marker	Allele	Peak (cM)	CI (cM)	LOD score	LOD score (s-level, $P = 0.05$)	Trait	References
EAE30	1	D1Mit380 D1Mit236	D1Mit303[a]	SJL/J	22	11–32	3.4[a] 4.7[b] 3.9[c]	3.5 4.7[b] 3.7[c]	Forelimb cMEP latency day 15	New, overlaps with Idd5 locus in diabetes, Greve *et al.* (16)
EAE31	8	D8Mit24 D8Mit88	D8Mit258 D8Mit259 D8Mit178 D8Mit15	SJL/J	42	32–48	6.9	3.7	Forelimb cMEP latency day 0	New
EAE32	15	D15Mit126 D15Mit35	D15Mit67 D15Mit171	C57BL/10.S	38	24–56	4.5 6.1[b]	3.8 5.6[b]	Hindlimb cMEP latency, difference day 15–day 0	New
EAE33	2	D2Mit11 D2Mit372	D2Mit32	C57BL/10.S	20	6–30	3.7	3.6	Severity females	New
EAE34	10 10	D10Mit2 D10Mit233	D10Mit233 D10Mit271	C57BL/10.S C57BL/10.S	56 59	42–58 52–58	3.8 3.7	3.6 3.5	Severity females Onset females	New, partially overlaps with EAE17, Blankenhorn *et al.* (17)
EAE35	18	D18Mit186.1	D18Mit144.1[a]	C57BL/10.S	68	54–69	3.26[a]	3.6	Severity females	Overlaps with EAE25, Blankenhorn *et al.* (17)
EAE36	8	D8Mit124 D8Mit178	D8Mit258 D8Mit259	SJL/J	26	2–34	4.1	3.6	T-lymphocytes infiltration in spinal cord	Overlaps with EAE14, Blankenhorn *et al.* (17)
EAE37	15	D15Mit171	D15Mit35	C57BL/10.S	69	58–69	3.6	3.5	Microglia infiltration in spinal cord	New
EAE38	15	D15Mit67.1 D15Mit35	D15Mit171[a]	C57BL/10.S C57BL/10.S	54 56	18–72 46–68	3.3[a] 3.3[a]	3.6 3.5	AUC males B-lymphocytes infiltration in spinal cord	New

CI, Confidence intervals; LOD score s-level, significance level 95% (threshold values calculated based on 1000 permutations).
[a]Suggestive locus.
[b]Sex influence.
[c]Severity influence.

We choose the latency of cMEP as a trait because it appeared to be the most reproducible and reliable parameter for both myelin disturbance and functional impairment. By doing this, we identified three EAE loci associated to this trait (Table 1; Fig. 1). A suggestive evidence of linkage on chromosome 1 (EAE 30) to marker D1Mit303 associated to the latency of cMEP 15 days after immunization (latency at day 15 recorded in the fore limb, LOD score of 3.4). The linkage became statistically significant only when severity as a covariance was used in the analysis (LOD 3.7, Fig. 1E).

A linkage on chromosome 8 (EAE 31) showed a high significance (peak marker D8Mit178, LOD score of 6.99). Surprisingly, the locus influenced the latency of cMEP in the fore limb before immunization. A third locus on chromosome 15 (marker D15Mit67, LOD score 4.5), identified as EAE 32, influenced the latency of cMEP 15 days after immunization. In this case, we use the difference in the latencies between days 0 (before immunization) and 15 as a trait and we recorded the cMEP in the hind limb. The same locus linked to disease severity in males.

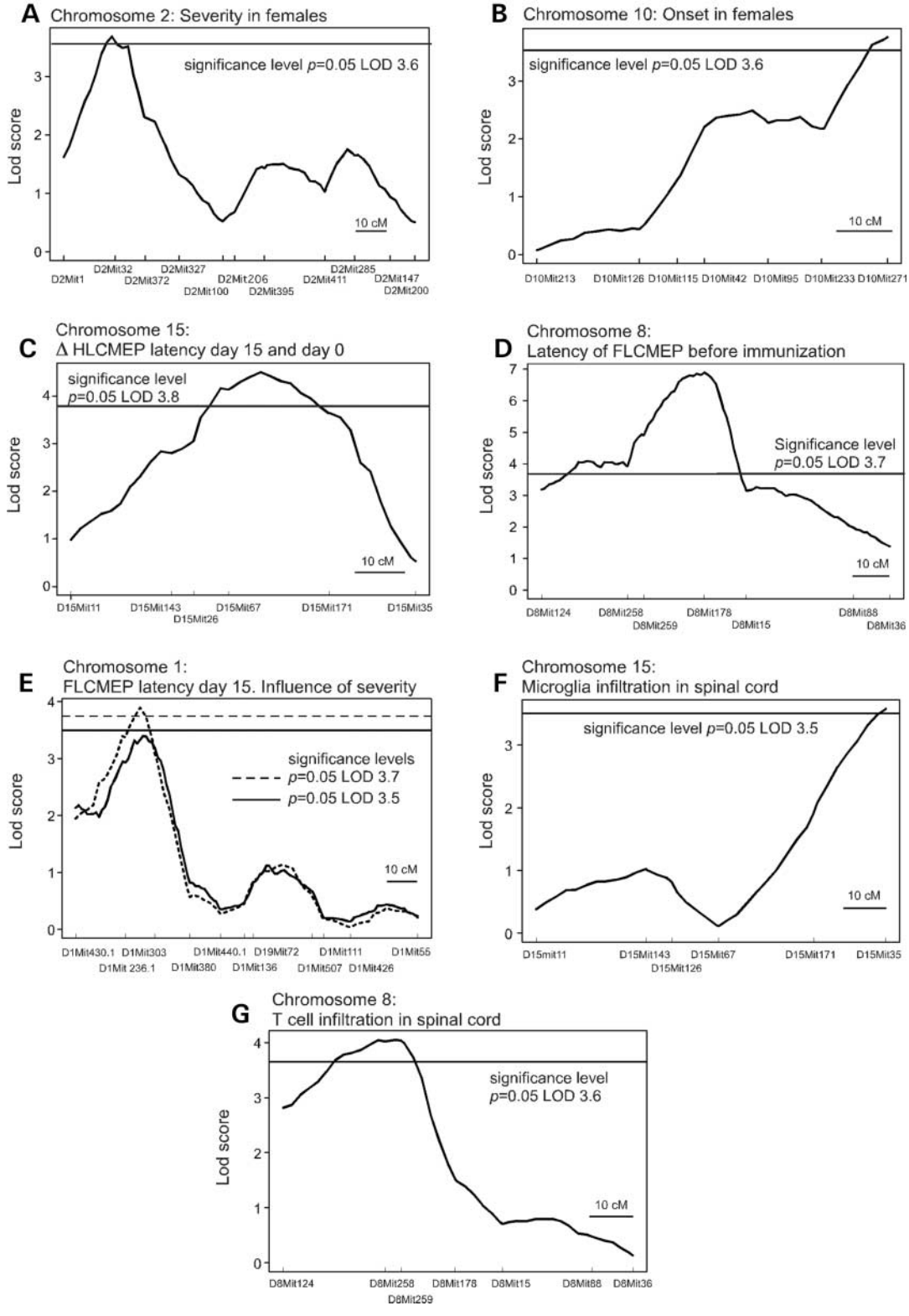

Figure 1. QTL identified in this study. QTL graphics showing the linkage between the different traits and the corresponding microsatellite marker. LOD score values represent the values for which each association became statistically significant (**A)** EAE 33 QTL associated to disease severity in females. (**B)** EAE 34 QTL linked to disease onset in females. (**C)** EAE 32 QTL associated to latency of cMEP in hind limb (HLCMEP) 15 days after immunization [trait study as a difference (Δ) between the latency at day 15 and the latency at day 0 for each mouse]. (**D)** EAE 31 QTL associated to latency of cMEP measured in the fore limb (FLCMEP) before immunization (day 0). (**E)** EAE 30 QTL associated to latency of cMEP measured in the fore limb 15 days post–immunization. Full lines represent the association graphic, whereas segment lines represent the association graphic using the severity as a covariant. (**F)** EAE 37 QTL linked to microglia infiltration in spinal cord. (**G)** EAE 36 QTL linked to T-cell infiltration in spinal cord.

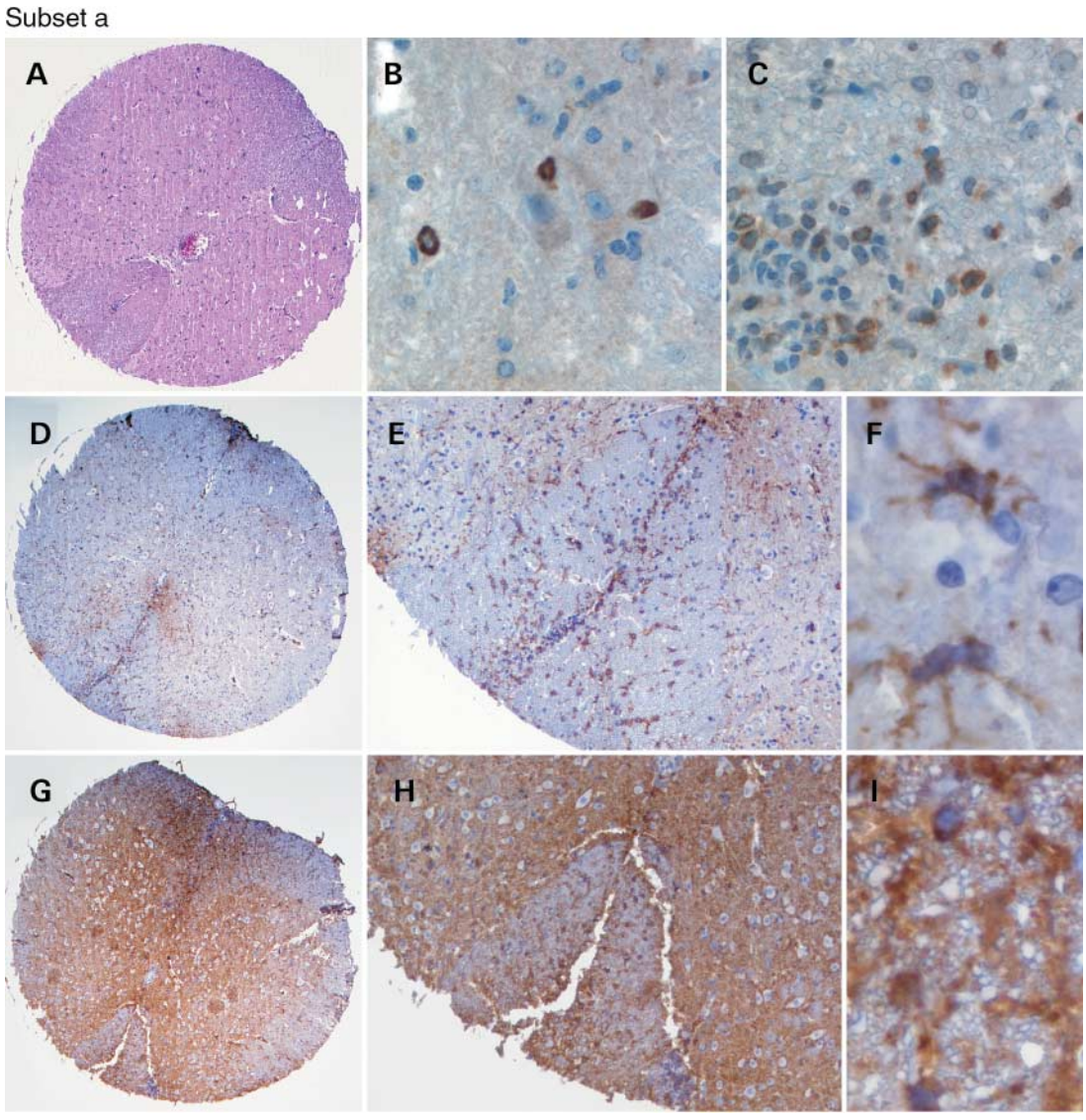

Figure 2. Morphological analysis of spinal cord cylinders arranged in TMAs. Subset a. (**A**) Hematoxilin–eosin stain (H&E) of a representative spinal cord cylinder of 1.3 mm diameter. (**B**) B-lymphocytes infiltration (B220, 20 ×). (**C**) T-lymphocytes infiltration (CD3, 20×). (**D**–**F**). Low microglia infiltration (IBA-1). (**G**–**I**). High microglia infiltration (IBA-1) [magnifications (D and E) 1×; (E and F) 5×; (F), I 40×]. Subset b. Myelination properties is represented in (A and B) and stain of the MBP and number of axons in (C and D). Neurofilament (NF200) axonal stain [magnifications (A and B) 1×; (B and D) 10×; left white matter, right gray matter]. Myelin and axonal stains revealed no significant individual differences between the mice.

There is no overlap between QTL controlling histopathological changes and QTL controlling cMEP latencies.

A decrease of the incidence in mice used for the electrophysiology (42%) when compared with the rest of F2 mice (58 %) was observed ($\chi^2 = 15.01 > 3.84$) but disease severity and onset were not affected by the neurological procedure. The mean disease severity score in mice for electrophysiology was 2.72 ± 1.50, which did not differ from the whole group, 2.67 ± 1.29 ($P = 0.8$). The mean onset values in the electrophysiological group and the whole group were 13.31 ± 3.19 and 12.98 ± 3.22 days, respectively ($P = 0.8$). To validate the loci, a two-point analysis (F-statistics, ANOVA) was performed (Supplementary Material, Table S2).

Association and correlation between QTLs influencing cMEP and incidence, disease onset, disease severity and cell infiltration

To explore the relevance of cMEP controlling alleles, we investigated their effect, i.e. their relationship to incidence onset and severity of disease, as well as to cell infiltration. EAE 30 influenced the latency of cMEP at day 15 as recorded in the fore limb and was associated to the incidence of the disease because sick mice at day 15 showed longer conduction times than healthy mice ($P = 0.02$) (Tables 3 and 4, Supplementary Material, Table S1 and Supplementary Material, Fig. S1). Additionally, mice with severe disease had longer latencies than healthy mice ($P = 0.009$). When we divided

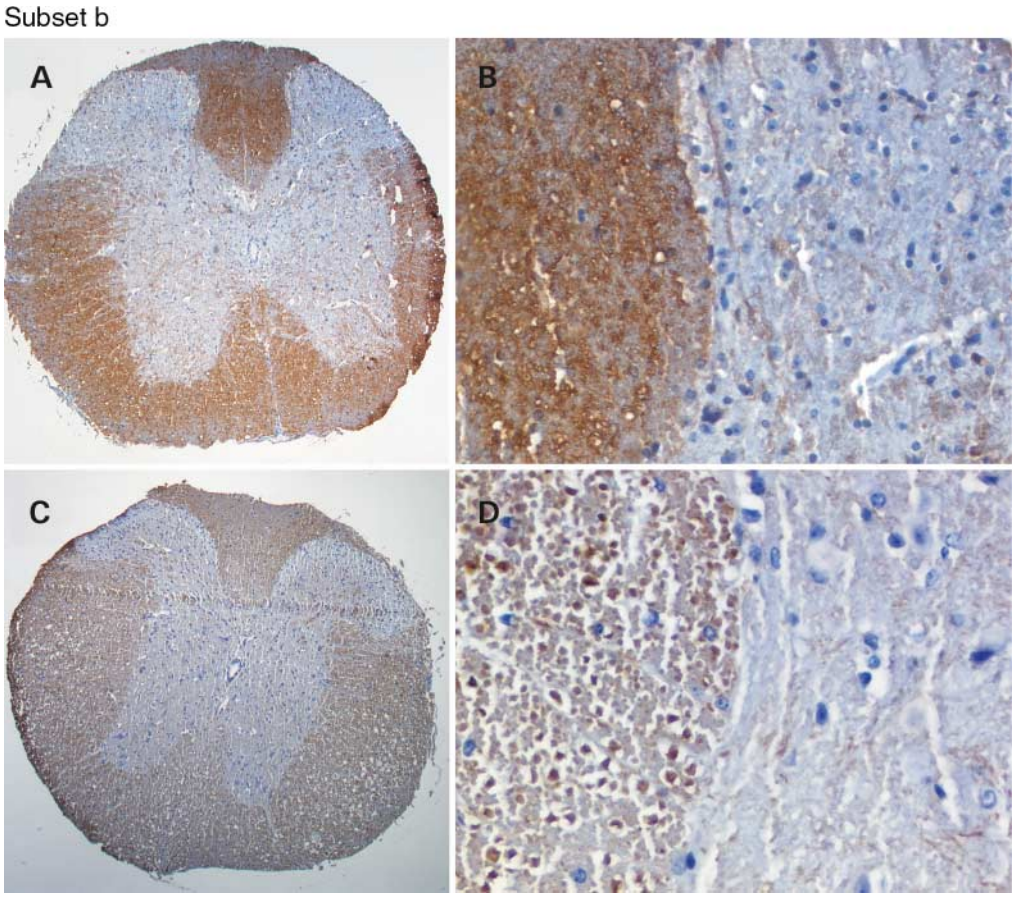

Figure 2. *Continued.*

the mice in groups, depending on their alleles at this locus, it was evident that the SJL allele is the major contributor to this association. In this case, mice with both mild and severe disease show differences with respect to healthy mice ($P = 0.036$ and $P < 0.001$, respectively). Furthermore, mice with the SJL allele at this locus, with B-lymphocyte infiltration in their spinal cords show slower conduction times than mice without infiltration ($P < 0.001$) (Supplementary Material, Fig. S2). EAE 31 linked to the fore limb cortical motor evoked potential (FLCMEP) latencies before immunization. This is reflected in the significant differences between the B10S and the SJL (D8Mit178) mice ($P < 0.001$). Mice with the SJL allele had longer latencies than mice with the B10S allele. Early onset associates with longer latencies ($P = 0.018$). However, there was no association between the latencies before immunization and the incidence or severity of the disease.

EAE 32 linked to the latency of cMEP in the hind limb was assessed by using the difference between the latencies at days 0 and 15 as a phenotype. The association of this trait with incidence of disease was very strong ($P < 0.001$) and was independent of the allele carried by the mice (Tables 3 and 4). We also observed differences in the latencies of cMEP between healthy mice with respect to mice suffering from mild disease and mice having severe disease (Table 4). There is an association with severity showing that mice with severe disease had longer conduction times than mice presenting mild symptoms ($P = 0.006$). Regression analysis (Table 3) showed a good correlation between disease severity in mice with the B10S allele in this locus and latency of cMEP ($R = 0.87$ for B10S allele homozygous mice and $R = 0.77$ for mice with at least one copy of the B10S allele). There is also an association with B-lymphocyte infiltration in spinal cords because the mice with infiltration showed slower conduction times (measured as a difference between day 0 and day 15) than mice without infiltration. Again, mice with at least one copy of the B10S allele at D15Mit67 locus and B-lymphocytes infiltration have longer conduction times than mice without B-lymphocyte infiltration (Supplementary Material, Fig. S2).

DISCUSSION

The most important finding of this study is the identification of three new QTLs controlling the latency of cMEPs, a phenotype that functionally reflects the disease activity and provides quantitative data additional to the semi-quantitative clinical severity data.

EAE 30 on chromosome 1, 11–32 cM, controlled the latency of cMEP, as recorded in the fore limb. The linkage was disease dependent, as significance was detected when using disease as a covariate in the analysis. This is concordant

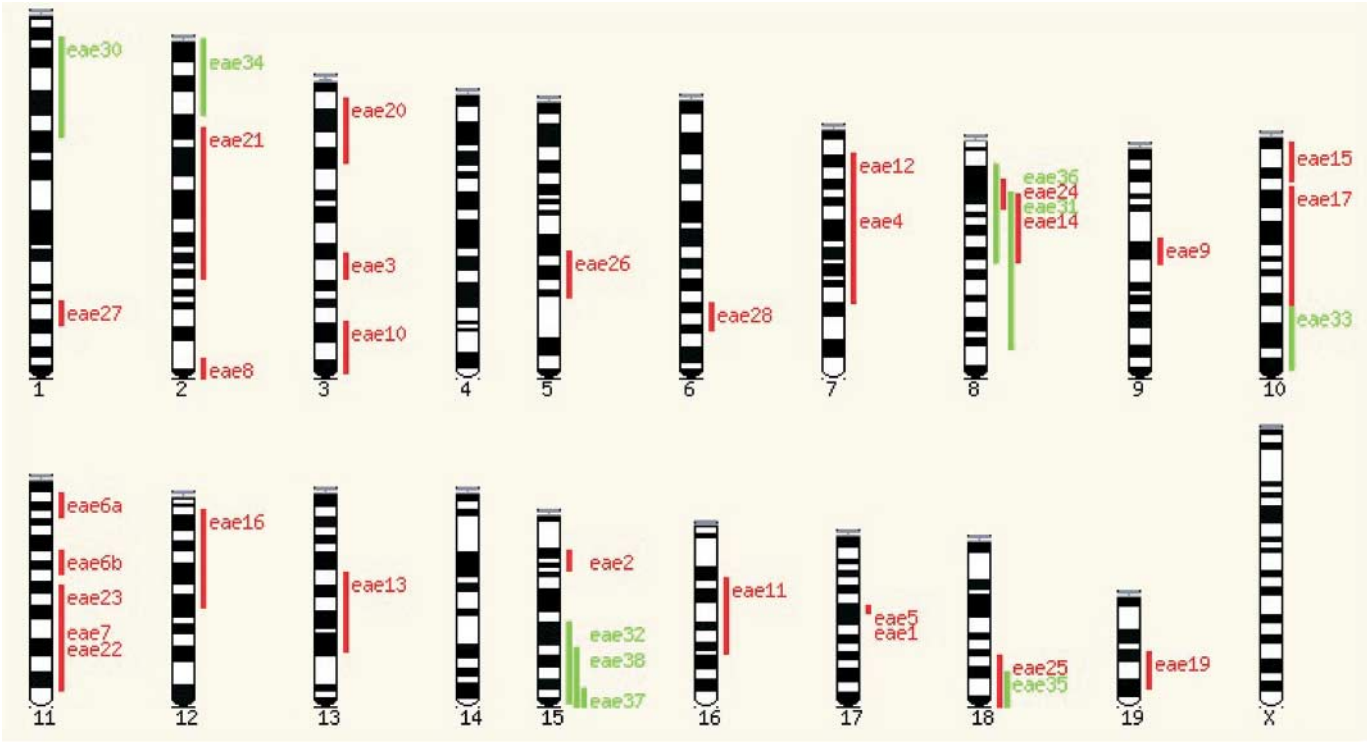

Figure 3. Comparison between published EAE loci and those QTL identified in this study. Red lines correspond to the 28 QTL described in the literature while green lines represent the QTL described in our study.

Table 2. Comparison of cMEP latencies between parental strains and F2 generation

Strain	Days post-inoculation	All mice fore limb (ms)	All mice hind limb (ms)	Females fore limb (ms)	Male fore limb (ms)	Female hind limb (ms)	Male hind limb (ms)
Parental							
C57BL/10.S	0	$2.57^{a} \pm 0.17$	$3.90^{a*} \pm 0.14$				
SJL/J	0	$2.71^{a} \pm 0.12$	$4.03^{a*} \pm 0.14$				
F2 generation (SJL/J × C57BL/10.S)	0	$2.66^{b,c} \pm 0.27$	$3.96^{b,c} \pm 0.29$	$2.63^{b,c} \pm 0.28$	$2.72^{b,c} \pm 0.24$	$3.88^{b,c} \pm 0.54$	$4.01^{b,c} \pm 0.27$
	10	$2.92^{b} \pm 0.32$	$4.13^{b,d} \pm 0.43$	$2.91^{b} \pm 0.33$	$2.94^{b} \pm 0.32$	$4.01^{b,d} \pm 0.57$	$4.27^{b} \pm 0.60$
	15	$3.00^{c} \pm 0.34$	$4.26^{c,d} \pm 1.29$	$2.95^{c} \pm 0.32$	$3.09^{c} \pm 0.38$	$4.26^{c,d} \pm 0.67$	$4.55^{c} \pm 1.26$
	Difference days 10 and 0	$0.27^{e} \pm 0.29$	$0.16^{e} \pm 0.46$	0.27 ± 0.31	0.23 ± 0.26	$0.11^{e} \pm 0.32$	0.28 ± 0.68
	Difference days 15 and 0	$0.37^{e} \pm 0.34$	$0.41^{e} \pm 0.89$	0.36 ± 0.32	0.39 ± 0.41	$0.33^{e} \pm 0.69$	0.59 ± 1.33

Values are given as mean ± SD.
[a]Significant differences between the strains, $P < 0.05$.
[b]Significant differences between days 0 and 10 post-immunization, $P < 0.05$.
[c]Significant differences between days 0 and 15 post-immunization, $P < 0.05$.
[d]Significant differences between days 10 and 15 post-immunization, $P < 0.05$.
[e]Significant differences between latencies (days 10–day 0) and latencies (days 15–day 0), $P < 0.05$.

with the observation that the latency of FLCMEP was enhanced in diseased mice when compared with healthy mice, with the SJL/J allele as the contributing allele. EAE 30 partially overlaps with an earlier described locus (Tmevd 6), which controls severity in Theiler's murine encephalomyelitis, a virus-induced demyelinating disease (12–14). It also overlaps with the Idd5a locus identified in the NOD mice as pre-disposing to diabetes (15), where there is strong evidence that CTLA4 and/or ICOS (16) are the likely susceptibility gene for this locus.

EAE 31 locus on chromosome 8, 32–48 cM, controlled the latency of cMEPs before immunization. As shown for the EAE 30, the contributing allele originated from the susceptible strain, SJL/J, and had a dominant effect. A longer latency of

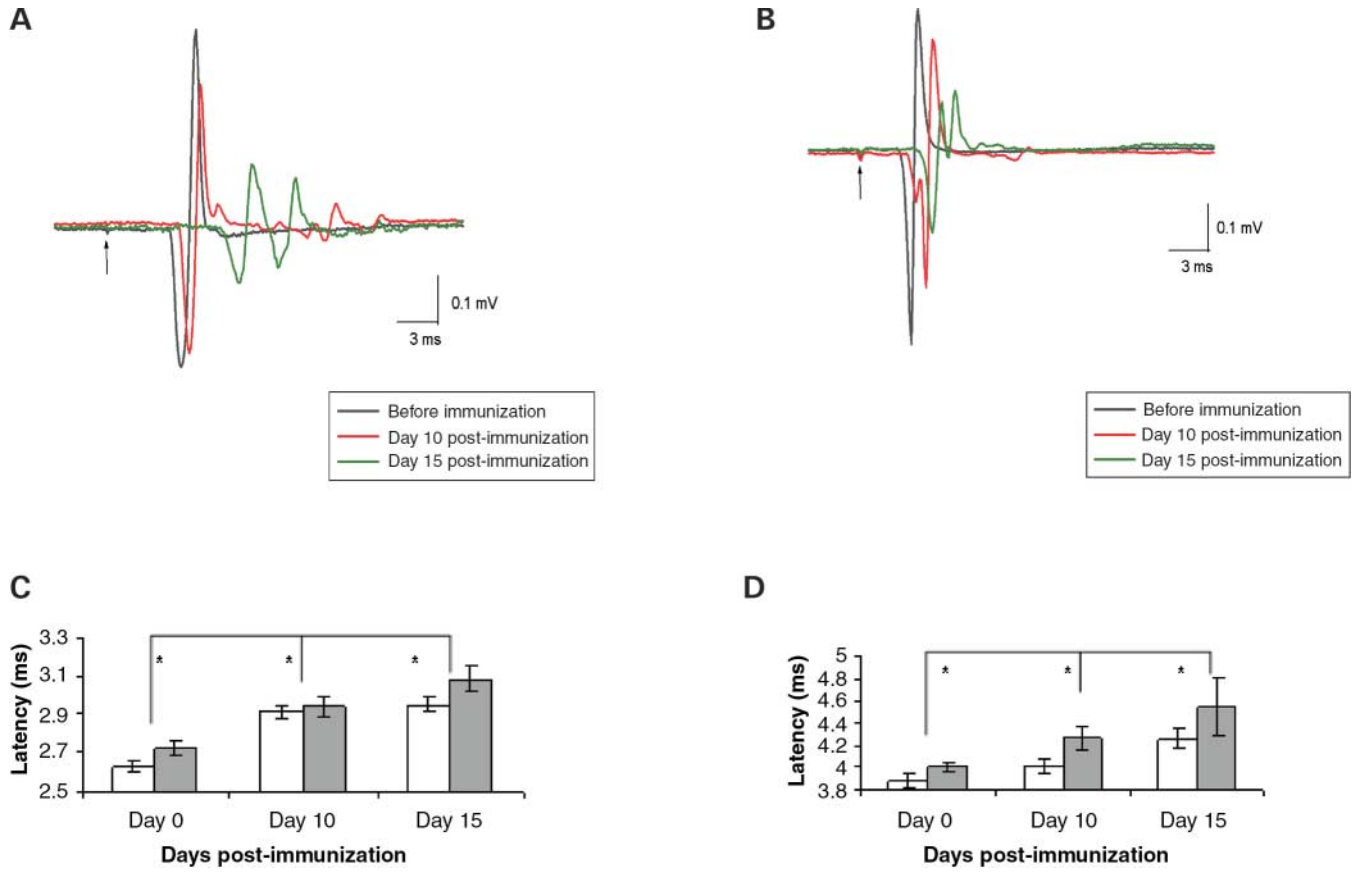

Figure 4. CMEP latencies—changes during the course of disease. Representative traces of cMEP recorded in (**A)** the hind limb and (**B)** the fore limb before immunization (gray), 10 days (red) and 15 days post-immunization (green) in a sick mouse. CMEP are overlayed for clarity. Arrows indicate the time point of stimulation. Note the progressive increment in latencies and the decomposition with time post-immunization. (**C** and **D).** Effect of sex and disease on the fore limb (C) and on the hind limb cMEP latencies (D). Black bars represent the mean values of the F2 male population at different time points (days 0, 10 and 15), whereas white bars represent the mean values of the F2 female mice. Significant differences in the latencies of fore limb and hind limb cMEP were observed in both groups, males and females, during the course of disease.

cMEPs (measured in the fore limb) before immunization also correlates significantly with an earlier onset of the disease ($P < 0.001$). This suggests that at least one gene affecting axon structure, myelin composition or synapse transmission may pre-dispose susceptible mice to an early onset of the disease. EAE 31 partially overlaps with the EAE 14 locus previously linked to the incidence (9) of the disease and to demyelination (17). EAE 31 maps to a region that also contains several genes of putative relevance. One of those genes, the calcium channel alpha1 subunit gene (CACNA1a), encodes the alpha subunit of a P-type calcium channel (18–20). CACNA1a is associated with neurological symptoms in mice, like ataxia. Furthermore, it is polymorphic and earlier studies show that it is differentially expressed during the course of EAE (21). Another interesting but less likely contributing gene, Caspase 3, is involved in apoptotic death of different neuronal cells (22–24) where apoptosis is one of the pathways that leads to demyelination (25). Genes like the Janus kinase 3 (JAK3) and carboxypeptidase E (CPE) are also putative contributors, although these genes cannot be linked to the phenotype studied. However, both genes mapped to this interval are differentially expressed during the disease (26) and are polymorphic genes (27–30). CPE is a secretory granule enzyme involved in dibasic cleavage of pro-proteins and pro-hormones (31), whereas JAK3 is a tyrosine kinase involved in signal transduction processes (32).

The association between the susceptibility allele on chromosome 8 with a slower conduction and with an earlier onset of disease could have an important meaning because such a predictive allele could be used to screen populations at high risk of developing MS by the non-invasive evoked potential measurements. This finding is supported by the fact that parental strain differences in cMEP latencies are already observed before immunization and are likely to be related to different myelin composition. Animals with attenuated biochemical properties of the myelin sheath may, therefore, be more prone to develop early EAE. The differences in cMEP measurements could unravel patients that show distinct alteration of the myelin sheath, and it might, therefore, be a tool for either treatment monitoring or even risk assessment.

EAE 32 on chromosome 15 controlled the latency of cMEPs measured in the hind limb (LOD score 4.5). Interestingly, the

Table 3. Linear regression correlation between latencies of cMEP with severity and onset

QTL	Trait	Locus	Genotype in locus (allele)	Severity[a] (R)	Onset[a] (R)
EAE30	Latency of fore limb cMEP 15 days post-immunization	D1Mit303	All mice	0.33	–
			C57BL/10.S	0.19	
			Heterozygous	0.01	
			SJL/J	0.37	
EAE31	Latency of fore limb cMEP before immunization	D8Mit178	All mice	−0.06	−0.42
			C57BL/10.S	−0.1	−0.198
			Heterozygous	−0.04	−0.30
			SJL/J	−0.07	−0.40
EAE32	Latency of hind limb cMEP day 15 (day 15−day 0)	D15Mit67	All mice	0.64	–
			C57BL/10.S	0.87	
			Heterozygous	0.76	
			SJL/J	−0.17	

[a]Correlation.

Table 4. Association between latencies of cMEP with severity, onset and incidence of disease[a]

QTL	Linkage marker	Effect allele	Sex effect	Genotypes in locus (allele)	Disease association	Severity association	Onset association
EAE30	D1Mit303	SJL/J	No	All mice	$P = 0.02$	No (healthy−mild) $P = 0.009$ (healthy−severe) No (mild−severe)	No
				C57BL/10.S	No	No	No
				Heterozygous	No	No	No
				SJL/J	$P < 0.001$	$P = 0.036$ (healthy−mild) $P < 0.001$ (healthy−severe) No (mild−severe)	No
EAE31	D8Mit178 $P < 0.001$	SJL/J Dominant	No	All mice	No	No	$P < 0.001$ (early-late)
	(C57BL/10.S-SJL/J) $P < 0.001$	effect		C57BL/10.S	No	No	No (early-late)
	(C57BL/10.S-hetero) $P = 0.05$			Heterozygous	No	No	$P = 0.03$ (early-late)
	(hetero-SJL/J)			SJL/J	No	No	No (early-late)
EAE32	D15Mit67 $P = 0.008$	C57BL/10.S Dominant effect	Yes	All mice	$P < 0.001$	$P = 0.008$ (healthy−mild) $P < 0.001$ (healthy−severe) $P = 0.006$ (mild−severe)	No
	(C57BL/10.S-SJL/J) $P = 0.046$			C57BL/10.S	$P = 0.05$	No (healthy−mild) $P < 0.001$ (healthy−severe) $P = 0.009$ (mild−severe)	No
	(C57BL/10.S-hetero) No			Heterozygous	$P = 0.003$	No (healthy−mild) $P < 0.001$ (healthy−severe) $P = 0.017$ (mild−severe)	No
	(hetero-SJL/J)			SJL/J	$P = 0.003$	$P = 0.001$ (healthy−mild) $P = 0.003$ (healthy−severe) No (mild−severe)	

[a]Statistical analysis by ANOVA.

C57BL/10.S allele was responsible for the delay of cMEPs after 15 days and had a dominant effect. The delay of the cMEPs correlated with the incidence disease severity and the B-lymphocyte infiltration. A candidate gene in this locus is the calcium channel gamma subunit gene (CACNG2), which encodes stargazing, a transmembrane protein, which may act as both neuronal voltage-dependent calcium channel gamma subunit and AMPA receptor regulatory proteins (TARPs) and is highly expressed in cerebellum, cerebral cortex, hippocampus and thalamus. CACNG2 is differentially expressed during EAE (21) and it has been associated with neurological disorders (33). Another interesting gene in this region is peripherin, an intermediate filament protein, which is upregulated in inflammatory processes and leads to a degeneration of motor axons in amyotrophic lateral sclerosis (34).

Our morphological analysis of the spinal cords of the F2 population did not reveal obvious differences in the myelination pattern, however, already minor changes in the biochemical composition of the isolating myelin sheath are known to influence the electrophysiological properties of spinal cord tracts. These biochemical changes may be explained by the inflammation produced by the cell infiltration because our study reveals an association between the cMEP latencies 15 days post-immunization with the B-lymphocyte infiltration. (Supplementary Material, Fig. S2)

In addition to the cMEP QTLs, we identified new QTLs controlling traits like disease severity, disease onset and cell infiltration.

Two new QTLs on chromosomes 2 (D2Mit32) and 10 (D10Mit271) were associated with severity in females (Table 1). EAE 34 is a new QTL, although it partially overlaps with EAE 17, which has previously been shown to be associated with disease severity and spinal cord demyelination in females (9). EAE 33 on chromosome 2 represents a new locus that is mapped to the distal p-fragment of the chromosome. This appears to be a common QTL for other autoimmune diseases e.g. collagen-induced arthritis (CIA2) (35). There is evidence suggesting that the complement C5 is the probable susceptibility gene in this area because many strains showing linkage to arthritis are C5 deficient due to a two base pair mutation. However, there are no known polymorphisms or mutations in the C5 gene in C57Bl/10 or SJL/J. This observation and additional evidence from arthritis linkage analysis studies suggest that other genes in this locus might be involved. On chromosome 18, we identified a suggestive QTL (EAE 35). This locus overlaps with the EAE 25, a QTL previously described as contributing to spinal cord lesions in EAE (17).

Onset of the disease was linked to D10Mit233, suggesting that the same QTL may influence severity and onset of the disease in our F2 study. Several genes of importance are mapped in this region like interferon gamma, a determinant factor of disease (36).

Furthermore, we describe two QTLs controlling for the infiltration of microglia and B-lymphocytes in a distal position on chromosome 15. The presence of both cell types is a sign of spinal cord inflammation and both cell types probably target myelin sheath epitopes. Recently, it was shown that microglia contact myelin membranes before the onset of demyelination, suggesting that this contact could lead to a later demyelination and inflammation (37). Indeed, microglia is the major effectors cell in the CNS, and cytokines like IFN-gamma and TNF activate microglia into migratory and phagocytic cells. However, there is also evidence for a role of extracellular matrix proteins as a regulator or modulator proteins of microglia activity probably by increasing the local accessibility of fibronectin due to different pathological conditions in the CNS, like MS (38), and this in turn induces microglia activation and expression of integrins like alpha-4-beta1 and alpha-5-beta1 integrin (37). Integrin alpha-5 (fibronectin receptor-alpha-5) maps at this region on chromosome 15. The fact that this region also associates to the severity in males supports the suggested role of this area in the development of the disease.

In conclusion, the cMEP-associated QTLs correlated with incidence, onset or severity of disease and did not overlap with QTL controlling cell infiltration, suggesting a possible role of genetic control of basic myelin composition or patterns and synaptic structure mediated by polymorphic genes on chromosomes 1, 8 and 15 in susceptibility to EAE. In addition, our data provide evidence for the view that not the entire functional impairment is reflected by observable morphological changes on light or electron microscopy level but rather strengthens the reliability of our new strategy to choose cMEPs as a trait for QTL analysis in diseases involving demyelination.

Further strategies must be done to confirm the role of these genes in EAE. Search for polymorphism in the candidate genes by sequencing, congenic or subcongenic strains generation for fine mapping, gene expression profiling in these QTL, comparative genomics or functional analyses by knock-out or transgenesis are some of the strategies that we are developing to point out the relevant genes in the disease.

MATERIALS AND METHODS

Mice, immunization and score of the disease

The mice used in this study were obtained from the Jackson Laboratory and were kept under standard laboratory conditions. The local state's Animal Care Committee previously approved all experimental procedures in agreement with the European Communities Council Directive of November 24, 1986 (86/609/EEC). We inoculate the disease according to established protocols (7). In brief, SJL/J, C57BL/10.S, (SJL/J × C57BL/10.S) F1 and 400 (SJL/J × C57BL/10.S) F2 mice were immunized at 8–12 weeks of age at the base of the tail with 100 μg of PLP139-151 (American Peptide Company, Sunnyvale, CA, USA) dissolved in water and mixed with an equal volume (50 μl) of CFA (IFA with 4 mg/ml *Mycobacterium tuberculosis*; DIFCO Laboratories Detroit, USA). 200 ng of *Bordetella pertussis* toxin (Sigma, St Louis, MO, USA) was injected to each mouse on the day of immunization and 48 h later. Mice were followed for 4 weeks post-immunization. The clinical scoring (severity) of EAE commenced 8 days after immunization and animals were monitored daily according to the current protocol: 0, norma1; 1, flaccid tail; 2, waddle; 3, moderate paraparesis; 4, severe paraparesis and 5, tetraparesis. We analyzed the severity as the maximal score observed in each individual mouse or the AUC, a continuous trait that measures the accumulative severity from the disease onset until the day of sacrifice. The day of onset was also analyzed as a quantitative trait.

CMEP recordings

We used a total of 15 mice of each parental strain (SJL/J and C57BL/10.S) and 125 (SJL/J × C57BL/10.S) F2 mice for electrophysiological analysis. The F2 mice were randomly chosen and divided into five groups. Ten days after immunization, we anesthetized the 125 F2 mice for surgery by intraperitoneal injection of avertin (1.7 mg/g), an anesthetic composed of 2,2,2-tribromoethanol (Sigma) and 2-methyl-2-butanol (Sigma). Subsequently, we placed the mice in a

conventional stereotactic head frame and inserted two stainless steel screws (AgnTho's, Lidingö, Sweden) 1.5 mm right of the midline and 1.5 mm behind the bregma suture, with the tip just above the pia mater (anode) and on the nasal bone (cathode), under sterile conditions (39). At days 0, 10 and 15 post-immunization, we anesthetized the mice and elicited cMEP by constant current anodal square wave pulses of 150 μs duration and a frequency of 0.2 Hz applied to the brain surface of the motor cortex by a stimulator (A320, World Precision Instruments, Berlin, Germany) triggered by LabView-based software (National Instruments, Austin, TX, USA). Intensity was adjusted to 1.5 times the level inducing threshold contraction (40). We recorded the electromyographic response by needle electrodes (Medtronic Functional Diagnostics, Skovlunde, Denmark) positioned in the small muscles of the fore limb and the hind limb proximal to the elbow (12) against a reference located at the dorsum pedis of the paw. We also placed a ground electrode subcutaneously between stimulating and recording electrodes. Three recording sessions were performed over a period of 15 days. Five to 10 traces for each time point and stimulation were recorded, and the shortest onset latency of the first deflection latency was taken as a measure of the conduction time of cMEP.

We filtered the data with a band pass between 30 Hz and 1.3 kHz and amplified with a gain of 1 V/mV by an EXT-10C amplifier (NPI Electronics, Tamm, Germany). Further digitalizing (at 10 kHz) and analysis were done using LabView-based software (National Instruments) on a standard PC computer.

DNA isolation and genotyping

The genomic DNAs used for genotyping the mice were isolated from a 1 cm tail clip by using standard isolation protocols (41). We genotyped by PCR amplification all F2 generation mice. We used 150 informative microsatellite markers covering the genome to the extent of 98% of the genome at ~10 cM inter-marker distance. The mean inter-marker distance ranged from 5.5 to 21.5 cM for the different chromosomes. The accuracy of our loci order and interval maps was verified by comparing the genetic map calculated from our data with the Mouse Genome Informatics map (www.jax.org). The protocol for the genotyping was as follows. Genomic DNA (20 ng) was amplified in a final volume of 10 μl containing Hot Start *Taq* polymerase (0.25 U) (QIAGEN, Hilden, Germany), primers (0.1 μM each) (Metabion GmbH, Planegg-Martinsried, Germany), 50 mM KCl, 1 mM Tris, 2.5 mM $MgCl_2$, 0.25 mM dNTP and 0.02 μM M13-IRD700 or M13-IRD800 (LI-COR, Inc., Lincoln, NE, USA). Amplification conditions were as follows: 95°C for 10 min, followed by two cycles of 94°C for 30 s, 59°C for 1 min, 72°C for 1 min, two cycles of 94°C for 30 s, 57°C for 1 min, 72°C for 1 min, then another 35 cycles of 94°C for 30 s, 55°C for 1 min, 72°C for 1 min and a final extension at 72°C for 7 min. The reactions were performed using GeneAmp PCR System 9700 cycler (Applied Biosystems, Inc., Foster City, CA, USA). The PCR products were resolved on denaturing polyacrylamide gels and were detected by using a LI-COR Model 4200L automated DNA sequencer (LI-COR). The genotypes were scored independently by at least two people using the Saga software supplied by LI-COR.

Morphology

Spinal cord tissue was arranged in two TMAs. TMAs were constructed as recently described (42). Shortly, multiple spinal cord sections of each animal were poured into a paraffin block. Spinal cord pieces were arranged in a TMA with 200 punch holes of 1.3 mm each. Spinal cord tissue cylinders of the mice were transferred from the initial block to the TMA using a puncher. Sections of 4 μm thickness were then transferred to epoxyd resin covered slides and pre-incubated in xylol for 2 h prior to the staining procedure. Slides were conventional stained with a Luxol–Nissl stain to highlight the myelin irregularities. A Ventana machine with the appropriate pre-treatment (0.1 M citrate or 1 mM EDTA) was used for immunohistochemical determination of damaged and regenerated axons, irregular myelin, demyelination and cell infiltration. Antibodies against APP (Boehringer, Mannheim, Germany), MBP (DAKO, Carpinteria, CA, USA), neurofilament (NF200) (Sigma), IBA1 (Wako Chemicals GmbH, Neuss, Germany), CD3 (LabVision, Freemont, CA, USA) and B220 (CD45R) (BDBiosciences, Heidelberg, Germany) were used. Slides were developed using the Ventana DAB MAP kit or the DAKO iView kit.

The staining was evaluated double blind by establishing a 1 to 5 point evaluation scale for the different staining intensities (Luxol–Nissl, APP, MBP and NF200). Staining intensity in control spinal cords was used as a reference. The number of CD3 and B220 positive cells was counted on a representative spinal cord diameter of 1.3 mm.

Linkage analysis

All linkage analyses have been performed using the imputation model in the R/qtl software package (43,44). The order of the loci was obtained from the mouse genome informatics database of the Jackson Laboratory (http://www.informatics.jax.org). EAE severity and onset of the disease, latencies of cMEP and spinal cord cell infiltration were taken as phenotypes. Continuous values were checked for normal distribution using QTL Cartographer Software and logarithmic values were used when necessary. For the significant and suggestive linkage threshold values, we have followed the guidelines for the permutation test of data (number of permutations = 1000), and significance level 95% ($P = 0.05$) was used to determine linkage. Intervals containing significant evidence of linkage were reanalyzed by using Analyse-it software (http://www.analyse-it.com) testing the association between marker and phenotype using analysis of variation (ANOVA).

Statistics

Results are expressed as mean ± SD or SEM where appropriate. A P-value <0.05 was considered significant. Linear regression and ANOVA were used to test the correlation or association between the latencies of cMEP and the onset, severity incidence of the disease and cell infiltration.

SUPPLEMENTARY MATERIAL

Supplementary Material is available at HMG Online.

ACKNOWLEDGEMENTS

The authors wish to thank Ilona Klamfuss and Eva Lorbeer for their technical assistances with the animals and Martina Storz for the assistance with TMAs. This work was supported by grants from BMBF (FKZ 01ZZ0108) and the University of Rostock.

Conflict of Interest statement. None declared.

REFERENCES

1. Ebers, G.C., Sadovnick, A.D. and Risch, N.J. (1995) A genetic basis for familial aggregation in multiple sclerosis. Canadian Collaborative Study Group. *Nature*, **377**, 150–151.
2. Dyment, D.A., Sadovnick, A.D., Ebers, G.C. and Sadnovich, A.D. (1997) Genetics of multiple sclerosis. *Hum. Mol. Genet.*, **6**, 1693–1698.
3. Teuscher, C., Hickey, W.F., Grafer, C.M. and Tung, K.S. (1998) A common immunoregulatory locus controls susceptibility to actively induced experimental allergic encephalomyelitis and experimental allergic orchitis in BALB/c mice. *J. Immunol.*, **160**, 2751–2756.
4. Kurtzke, J.F. (1993) Epidemiologic evidence for multiple sclerosis as an infection. *Clin. Microbiol. Rev.*, **6**, 382–427.
5. Serrano-Fernández, P., Ibrahim, S.M., Zettl, U.K., Thiesen, H.J., Gödde, R., Epplen, J.T.and Möller, S. (2004) Intergenomic consensus in multifactorial inheritance loci: the case of multiple sclerosis. *Genes Immun.*, **5**, 615–620.
6. Wandstrat, A. and Wakeland, E. (2001) The genetics of complex autoimmune diseases: non-MHC susceptibility genes. *Nat. Immunol.*, **2**, 802–809.
7. Encinas, J.A., Lees, M.B., Sobel, R.A., Symonowicz, C., Greer, J.M., Shovlin, C.L., Weiner, H.L., Seidman, C.E., Seidman, J.G. and Kuchroo, V.K. (1996) Genetic analysis of susceptibility to experimental autoimmune encephalomyelitis in a cross between SJL/J and B10.S mice. *J. Immunol.*, **157**, 2186–2192.
8. Bergsteinsdottir, K., Yang, H.T., Pettersson, U. and Holmdahl, R. (2000) Evidence for common autoimmune disease genes controlling onset, severity, and chronicity based on experimental models for multiple sclerosis and rheumatoid arthritis. *J. Immunol.*, **164**, 1564–1568.
9. Butterfield, R.J., Blankenhorn, E.P., Roper, R.J., Zachary, J.F., Doerge, R.W. and Teuscher, C. (2000) Identification of genetic loci controlling the characteristics and severity of brain and spinal cord lesions in experimental allergic encephalomyelitis. *Am. J. Pathol.*, **157**, 637–645.
10. Butterfield, R.J., Sudweeks, J.D., Blankenhorn, E.P., Korngold, R., Marini, J.C., Todd, J.A., Roper, R.J. and Teuscher, C. (1998) New genetic loci that control susceptibility and symptoms of experimental allergic encephalomyelitis in inbred mice. *J. Immunol.*, **161**, 1860–1867.
11. Klein, J., Figueroa, F. and David, C.S. (1983) H-2 haplotypes, genes and antigens: second listing. II. The H-2 complex. *Immunogenetics*, **17**, 553–596.
12. Iuliano, B.A., Schmelzer, J.D., Thiemann, R.L., Low, P.A. and Rodriguez, M. (1994) Motor and somatosensory evoked potentials in mice infected with Theiler's murine encephalomyelitis virus. *J. Neurol. Sci.*, **123**, 186–194.
13. McGavern, D.B., Murray, P.D., Rivera-Quinones, C., Schmelzer, J.D., Low, P.A. and Rodriguez, M. (2000) Axonal loss results in spinal cord atrophy, electrophysiological abnormalities and neurological deficits following demyelination in a chronic inflammatory model of multiple sclerosis. *Brain*, **123**, 519–531.
14. Butterfield, R.J., Roper, R.J., Rhein, D.M., Melvold, R.W., Haynes, L., Ma, R.Z., Doerge, R.W. and Teuscher, C. (2003) Sex-specific quantitative trait loci govern susceptibility to Theiler's murine encephalomyelitis virus-induced demyelination. *Genetics*, **163**, 1041–1046.
15. Wicker, L.S., Chamberlain, G., Hunter, K., Rainbow, D., Howlett, S., Tiffen, P., Clark, J., Gonzalez-Munoz, A., Cumiskey, A.M., Rosa, R.L. *et al.* (2004) Fine mapping, gene content, comparative sequencing, and expression analyses support Ctla4 and Nramp1 as candidates for Idd5.1 and Idd5.2 in the nonobese diabetic mouse. *J. Immunol.*, **173**, 164–173.
16. Greve, B., Vijayakrishnan, L., Kubal, A., Sobel, R.A., Peterson, L.B., Wicker, L.S. and Kuchroo, V.K. (2004) The diabetes susceptibility locus Idd5.1 on mouse chromosome 1 regulates ICOS expression and modulates murine experimental autoimmune encephalomyelitis. *J. Immunol.*, **173**, 157–163.
17. Blankenhorn, E.P., Butterfield, R.J., Rigby, R., Cort, L., Giambrone, D., McDermott, P., McEntee, K., Solowski, N., Meeker, N.D., Zachary, J.F. *et al.* (2000) Genetic analysis of the influence of pertussis toxin on experimental allergic encephalomyelitis susceptibility: an environmental agent can override genetic checkpoints. *J. Immunol.*, **164**, 3420–3425.
18. Doyle, J., Ren, X., Lennon, G. and Stubbs, L. (1997) Mutations in the Cacnl1a4 calcium channel gene are associated with seizures, cerebellar degeneration, and ataxia in tottering and leaner mutant mice. *Mamm. Genome*, **8**, 113–120.
19. Burgess, D.L. and Noebels, J.L. (1999) Single gene defects in mice: the role of voltage-dependent calcium channels in absence models. *Epilepsy Res.*, **36**, 111–122.
20. Lee, Y.C., Chen, J.T., Liao, K.K., Wu, Z.A. and Soong, B.W. (2003) Prolonged cortical relay time of long latency reflex and central motor conduction in patients with spinocerebellar ataxia type 6. *Clin. Neurophysiol.*, **114**, 458–462.
21. Carmody, R.J., Hilliard, B., Maguschak, K., Chodosh, L.A. and Chen, Y.H. (2002) Genomic scale profiling of autoimmune inflammation in the central nervous system: the nervous response to inflammation. *J. Neuroimmunol.*, **133**, 95–107.
22. Keramaris, E., Stefanis, L., MacLaurin, J., Harada, N., Takaku, K., Ishikawa, T., Taketo, M.M., Robertson, G.S., Nicholson, D.W., Slack, R.S. *et al.* (2000) Involvement of caspase 3 in apoptotic death of cortical neurons evoked by DNA damage. *Mol. Cell. Neurosci.*, **15**, 368–379.
23. Cid, C., Alvarez-Cermeno, J.C., Regidor, I., Plaza, J., Salinas, M. and Alcazar, A. (2003) Caspase inhibitors protect against neuronal apoptosis induced by cerebrospinal fluid from multiple sclerosis patients. *J. Neuroimmunol.*, **136**, 119–124.
24. Neumar, R.W., Xu, Y.A., Gada, H., Guttmann, R.P. and Siman, R. (2003) Cross-talk between calpain and caspase proteolytic systems during neuronal apoptosis. *J. Biol. Chem.*, **278**, 14162–14167.
25. Howe, C.L., Bieber, A.J., Warrington, A.E., Pease, L.R. and Rodriguez, M. (2004) Antiapoptotic signaling by a remyelination-promoting human antimyelin antibody. *Neurobiol. Dis.*, **15**, 120–131.
26. Ibrahim, S.M., Mix, E., Bottcher, T., Koczan, D., Gold, R., Rolfs, A. and Thiesen, H.J. (2001) Gene expression profiling of the nervous system in murine experimental autoimmune encephalomyelitis. *Brain*, **124**, 1927–1938.
27. Chen, H., Jawahar, S., Qian, Y., Duong, Q., Chan, G., Parker, A., Meyer, J.M., Moore, K.J., Chayen, S., Gross, D.J. *et al.* (2001) Missense polymorphism in the human carboxypeptidase E gene alters enzymatic activity. *Hum. Mutat.*, **18**, 120–131.
28. Utsunomiya, N., Ohagi, S., Sanke, T., Tatsuta, H., Hanabusa, T. and Nanjo, K. (1998) Organization of the human carboxypeptidase E gene and molecular scanning for mutations in Japanese subjects with NIDDM or obesity. *Diabetologia*, **41**, 701–705.
29. Haegeman, A., Williams, J.L., Law, A., van Zeveren, A. and Peelman, L.J. (2003) Mapping and SNP analysis of bovine candidate genes for meat and carcass quality. *Anim. Genet.*, **34**, 349–353.
30. Schumacher, R.F., Mella, P., Badolato, R., Fiorini, M., Savoldi, G., Giliani, S., Villa, A., Candotti, F., Tampalini, A., O'Shea, J.J. *et al.* (2000) Complete genomic organization of the human JAK3 gene and mutation analysis in severe combined immunodeficiency by single-strand conformation polymorphism. *Hum. Genet.*, **106**, 73–79.
31. Cool, D.R., Normant, E., Shen, F., Chen, H.C., Pannell, L., Zhang, Y. and Loh, Y.P. (1997) Carboxypeptidase E is a regulated secretory pathway sorting receptor: genetic obliteration leads to endocrine disorders in Cpe(fat) mice. *Cell*, **88**, 73–83.
32. Witthuhn, B.A., Silvennoinen, O., Miura, O., Lai, K.S., Cwik, C., Liu, E.T. and Ihle, J.N. (1994) Involvement of the Jak-3 Janus kinase in signalling by interleukins 2 and 4 in lymphoid and myeloid cells. *Nature*, **370**, 153–157.

33. Letts, V.A., Felix, R., Biddlecome, G.H., Arikkath, J., Mahaffey, C.L., Valenzuela, A., Bartlett, F.S., II, Mori, Y., Campbell, K.P. and Frankel, W.N. (1998) The mouse stargazer gene encodes a neuronal Ca2 + -channel gamma subunit. *Nat. Genet.*, **19**, 340–347.
34. Beaulieu, J.M., Nguyen, M.D. and Julien, J.P. (1999) Late onset of motor neurons in mice overexpressing wild-type peripherin. *J. Cell. Biol.*, **147**, 531–544.
35. McIndoe, R.A., Bohlman, B., Chi, E., Schuster, E., Lindhardt, M. and Hood, L. (1999) Localization of non-Mhc collagen-induced arthritis susceptibility loci in DBA/1j mice. *Proc. Natl Acad. Sci. USA*, **96**, 2210–2214.
36. Olsson, T. (1992) Cytokines in neuroinflammatory disease: role of myelin autoreactive T cell production of interferon-gamma. *J. Neuroimmunol.*, **40**, 211–218.
37. Milner, R. and Campbell, I.L. (2003) The extracellular matrix and cytokines regulate microglial integrin expression and activation. *J. Immunol.*, **170**, 3850–3858.
38. Venstrom, K.A. and Reichardt, L.F. (1993) Extracellular matrix. 2: role of extracellular matrix molecules and their receptors in the nervous system. *FASEB J.*, **7**, 996–1003.
39. Duckers, H.J., van Dokkum, R.P., Verhaagen, J., Lopes da Silva, F.H. and Gispen, W.H. (1996) Functional and neurophysiological evidence of the efficacy of trophic pharmacotherapy using an adrenocorticotrophic hormone 4–9 analog in experimental allergic encephalomyelitis, an animal model of multiple sclerosis. *Neuroscience*, **71**, 507–521.
40. Onofrj, M., Gambi, D., Bazzano, S., Colamartino, P., Fulgente, T., Malatesta, G. and Ferracci, F. (1992) Evoked potentials (EPs) in experimental allergic encephalomyelitis: a study of EP modifications during the course of a controlled disease. *Electromyogr. Clin. Neurophysiol.*, **32**, 125–135.
41. Laird, P.W., Zijderveld, A., Linders, K., Rudnicki, M.A., Jaenisch, R. and Berns, A. (1991) Simplified mammalian DNA isolation procedure. *Nucleic. Acids Res.*, **19**, 4293.
42. Moch, H., Schraml, P., Bubendorf, L., Mirlacher, M., Kononen, J., Gasser, T., Mihatsch, M.J., Kallioniemi, O.P. and Sauter, G. (1999) High-throughput tissue microarray analysis to evaluate genes uncovered by cDNA microarray screening in renal cell carcinoma. *Am. J. Pathol.*, **154**, 981–986.
43. Sen, S. and Churchill, G.A. (2001) A statistical framework for quantitative trait mapping. *Genetics*, **159**, 371–387.
44. Broman, K.W., Wu, H., Sen, S. and Churchill, G.A. (2003) R/qtl: QTL mapping in experimental crosses. *Bioinformatics*, **19**, 889–890.